Physics Letters A 380 (2016) 2237–2241

Contents lists available at ScienceDirect

Physics Letters A

www.elsevier.com/locate/pla

Kondo effect in magnetic tunnel junctions with an AlO_x tunnel barrier

Chao Zheng [a], Robert D. Shull [b], P.J. Chen [b], Philip W.T. Pong [a,*]

[a] *Department of Electrical and Electronic Engineering, The University of Hong Kong, Hong Kong*
[b] *Functional Nanostructured Materials Group, National Institute of Standards and Technology, Gaithersburg, MD 20899-8552, United States*

A R T I C L E   I N F O

Article history:
Received 23 February 2016
Received in revised form 29 April 2016
Accepted 1 May 2016
Available online 4 May 2016
Communicated by R. Wu

Keywords:
Kondo effect
Magnetic tunnel junction
Magnetization configuration
Spin-flip scattering

A B S T R A C T

The influence of the magnetization configuration on the Kondo effect in a magnetic tunnel junction is investigated. In the parallel configuration, an additional resistance contribution (R^*) below 40 K exhibits a logarithmic temperature dependence, indicating the presence of the Kondo effect. However, in the anti-parallel configuration, the Kondo-effect-associated spin-flip scattering has a nontrivial contribution to the tunneling current, which compensates the reduction of the current directly caused by Kondo scattering, making R^* disappear. These results indicate that suppression and restoration of the Kondo effect can be experimentally achieved by altering the magnetization configuration, enhancing our understanding of the role of the Kondo effect in spin-dependent transport.

1. Introduction

When dilute magnetic impurities are embedded in a metallic host, spin-flip scattering between the conduction electrons and the magnetic impurities gives rise to a logarithmic temperature dependence of the resistance of the system below a characteristic temperature, which is known as the Kondo effect [1]. The Kondo effect has been observed in various mesoscopic systems, including quantum dots [2,3], single-molecule transistors [4], non-local spin valves [5], and magnetic-doped thin films [6], *etc.* Though the Kondo effect has been intensively investigated, only a few studies focused on the influence of the Kondo effect on the transport behavior in magnetic tunnel junctions (MTJs). An unusual suppression of the tunneling magnetoresistance (TMR) of the MTJs was observed at low temperature and proved to be a result of the Kondo effect [7,9]. This observed manifestation of the Kondo effect was nearly independent of the magnetization alignment of the ferromagnetic layers in the published literature [7,9]. However, since the contributions of spin-flip scattering to the tunneling current in the parallel (P) and anti-parallel (AP) magnetization configurations are opposite [10], the Kondo effect is expected to be dependent on the magnetization configuration. More investigations are therefore required to explain this controversial issue.

In this work, the temperature dependence of the transport properties of MTJs is reported, providing experimental evidence for the presence of the Kondo effect in the MTJs. The main properties (spin, concentration, position) of the magnetic impurities are discussed. The influence of the magnetization alignment on the Kondo effect is investigated and explained by considering the spin-flip nature of the Kondo effect and its impact on the spin-dependent tunneling process.

2. Material and methods

The MTJ thin film was deposited using magnetron sputtering with a base pressure of 2.66×10^{-7} Pa. The structure of the MTJ thin film (units in nanometers) was as follows: substrate/10.0 NiFeCuMoTa/1.0 CoFe + pre-oxidization, $O_2 = 0.133$ Pa, 30 s/0.8 Al + plasma oxidization, $O_2 = 0.133$ Pa, 30 W, 30 s/1.0 CoFe/2.5 NiFeCuMoTa/0.5 CoFe/10.0 IrMn/7.0 Ru. Before deposition of the tunnel barrier, the pre-oxidization of the CoFe layer was performed in order to quench any orange-peel coupling [11]. The CoFe layer was oxidized by exposing it to a pure O_2 gas with pressure of 0.133 Pa for 30 s. The AlO_x tunnel barrier was formed by depositing an Al layer and subsequently oxidizing it in a pure O_2 plasma with pressure of 0.133 Pa and power of 30 W for 30 s. After the multilayer structure was prepared, the sample was annealed at 200 °C for 15 min in an in-plane magnetic field of 70 mT. After being annealed with desired duration, the sample was cooled naturally to room temperature and the applied magnetic field remained constant during the whole process. The MTJ thin film was then patterned to elliptical junctions with areas of 70 μm^2, 125 μm^2, 165 μm^2, and 190 μm^2 respectively using photolithography combined with etching processes. The transport behavior in the junctions was investigated using a four-probe technique and the magnetic field was applied along the easy axis of the MTJ.

---

* Corresponding author. Tel.: +852 2857 8491; fax: +852 2559 8738.
E-mail address: ppong@eee.hku.hk (P.W.T. Pong).

http://dx.doi.org/10.1016/j.physleta.2016.05.001
0375-9601/© 2016 Elsevier B.V. All rights reserved.

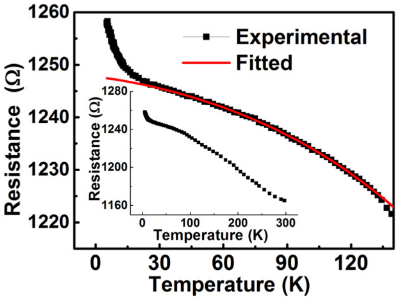

Fig. 1. Temperature dependence of R_P of the MTJ with junction area of 125 μm^2 measured from 140 K to 5 K. The red solid line is the fitted curve using the GM model, $R_P(T) = 1/G_P(T) = 1/(A + BT^{1.33} + CT^{2.5} + DT^{3.6})$, where G_P is the corresponding conductance in the P state, the fitting parameters $A = 8.02 \times 10^{-4}$ Ω^{-1}, $B = 1.40 \times 10^{-8}$ $\Omega^{-1}\,K^{-1.33}$, $C = 1.09 \times 10^{-11}$ $\Omega^{-1}\,K^{-2.5}$, and $D = 6.95 \times 10^{-14}$ $\Omega^{-1}\,K^{-3.6}$. Inset: temperature dependence of R_P measured from 300 K to 5 K. (For interpretation of the references to color in this figure legend, the reader is referred to the web version of this article.)

Temperature-dependent measurements were carried out in a cryostat over a temperature range from 300 K to 5 K, with temperature stability of ±0.1 K.

3. Results and discussion

The temperature dependence of the MTJ resistance was investigated and compared with the Glazman–Matveev (GM) hopping model [12]. A typical curve of the resistance (R_P) in the P magnetization alignment and its numerical fitting are shown in Fig. 1. The GM model can well reproduce the temperature dependence of R_P above 40 K. Below this critical temperature, R_P starts to deviate from the fitted curve and tends to be highly temperature-dependent, indicating the occurrence of an additional resistance contribution at low temperature. This additional resistance (R^*) is calculated by subtracting the fitted values from the experimental data. As shown in Fig. 2(a), R^* is negligible and exhibits no obvious change before temperature is decreased to about 40 K. Upon further reduction in temperature, R^* begins to increase and becomes more significant as temperature continues to decrease. This behavior presumably originates from the spin-exchange scattering interaction between the conduction electrons and the magnetic impurities, known as the Kondo effect [8,13].

To verify the above assumption, the R^* data are fitted by the Kondo empirical expression [14],

$$R^*(T) = R_0\left(\frac{T_0^2}{T^2 + T_0^2}\right)^S, \qquad T_0 = T_K\left(2^{\frac{1}{S}} - 1\right)^{-\frac{1}{2}} \tag{1}$$

R_0 represents the value of $R^*(T)$ extrapolated at 0 K, S is a dimensionless parameter, and T_K is the Kondo temperature, satisfying the equation $R^*(T_K) = R_0/2$. Fig. 2(b) shows the plot of the normalized resistance $R^*(T)/R_0$ with respect to the normalized temperature T/T_K and the fitted curve. The trend of $R^*(T)/R_0$ closely resembles the empirical expression with the fitting parameters $S = 1.71$, $T_K = 7.15$ K, and $R_0 = 16.14$ Ω. The logarithmic temperature dependence of $R^*(T)/R_0$ provides strong evidence for the presence of the Kondo effect in the MTJ [7,9,15].

The above manifestation of the Kondo effect is intimately related to the magnetic impurities in the system. By comparing the aforementioned fitting parameters (S, R_0) with those reported in the literature, the main properties of the magnetic impurities in the MTJs were analyzed. The value of S depends on the total spin of the magnetic impurity [16] and often varies distinctively among different types of systems [9,16,17]. The fitted S (1.71) in this work is much larger than that in a conventional spin-1/2 quantum dot system ($S = 0.22$) [14], suggesting the larger total spin values (>1/2) of the magnetic impurities in the MTJ that we are studying. However, a similar S (1.7) parameter was reported by J.H. Park's group in [9], where after one ferromagnetic layer (CoFe) was deposited, one more lightly-oxidized CoFe layer was formed using Ar mixed with a small amount of O_2 as the sputtering gas. Extra magnetic impurities (aluminum ferrite, $Al_{1+x}Fe_{1-x}O_{3+\delta}$) were believed to be formed between the AlO_x and CoFe layers, which was proved in their previous work [7]. In this MTJ, a pre-oxidization process was conducted after the deposition of the CoFe free layer, which also resulted in the formation of a lightly-oxidized CoFe layer on the top. Therefore, the aluminum ferrite could also be formed due to interlayer diffusion between the free layer and the barrier in this MTJ. The similar S parameters further suggest that the formed magnetic impurities reported in this study and [9] have similar values of the total spin. Furthermore, the concentration of magnetic impurities in MTJs can be qualitatively evaluated utilizing the correlation between the impurity concentration and the Kondo resistivity. The normalized Kondo resistivity at 0 K is defined as ρ_0. ρ_0 is closely related to the Kondo scattering rate, which is proportional to the concentration of magnetic impurities [6,18,19]. The estimated ρ_0 (∼3 Ωm) is much smaller than that (6.25×10^5 Ωm to 8.63×10^5 Ωm) in [9], indicating a much lower concentration of magnetic impurities in our MTJ. Compared with the pre-oxidization performed after the deposition of the free layer in our fabrication process, a larger amount of O_2 can penetrate into the ferromagnetic layer during deposition in [9], leading to the formation of magnetic impurities with higher concentration.

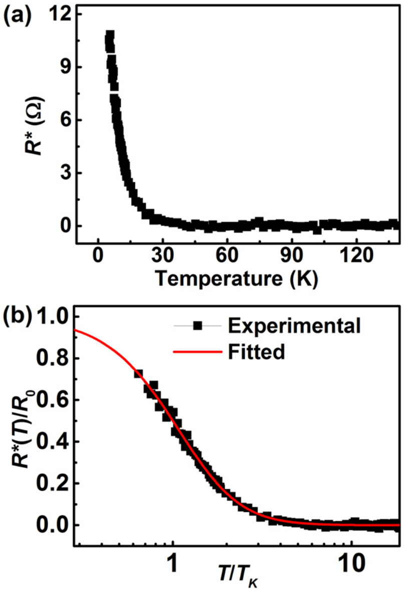

Fig. 2. (a) Temperature dependence of R^* of the MTJ with junction area of 125 μm^2. (b) Normalized resistance $R^*(T)/R_0$ as a function of the normalized temperature T/T_K. The red solid line is the fitted curve according to the Kondo empirical formula with the fitting parameters $S = 1.71$, $T_K = 7.15$ K, and $R_0 = 16.14$ Ω. (For interpretation of the references to color in this figure legend, the reader is referred to the web version of this article.)

To further verify the above discussion of magnetic impurities, the temperature dependence of R_P was investigated on several MTJs, each with a different junction area. $R^*(T)$ is also fitted by the empirical formula and the fitting parameters are extracted from the fitted curve. Almost the same S (∼1.7) and ρ_0 (∼3 Ωm) values are obtained for all MTJs, as exhibited in Fig. 3. This is expected because all MTJs are patterned on the same wafer, therefore both the type and concentration of magnetic impurities in all MTJs would be expected to be similar.

The location of magnetic impurities was also investigated by analyzing the trend of $R^*(T)$ as well as the temperature depen-

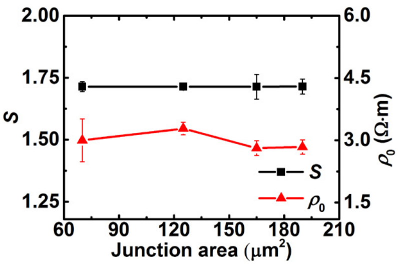

Fig. 3. Fitting parameters S and ρ_0 as a function of junction area. Based on the Kondo empirical formula, the parameters are extracted from the fitted curve ($R^*(T)/R_0$ versus T/T_K) for each MTJ using the same fitting procedure. The measured MTJs are divided into 4 groups each with a different junction area (70 μm^2, 125 μm^2, 165 μm^2, and 190 μm^2). Each data point is averaged from 4 MTJs with the same junction area. The error bars in the figure represent one standard deviation from the mean.

dence of the squareness of magnetic transfer curves. The $R^*(T)$ manifestation of the Kondo effect is highly dependent on the position of magnetic impurities [7,9,10]. When the magnetic impurities are formed in the ferromagnetic layer or at the interface between one ferromagnetic layer and the barrier, the conduction electrons tend to be scattered by these impurities, giving rise to an increase of the resistance [7,9]. When the magnetic impurities are formed inside the barrier, additive resonant channels are possibly activated, resulting in a reduction in the junction resistance [10,20]. The rapid rise of the resistance in this MTJ is consistent with the former case. In order to further determine whether the impurities are formed in the ferromagnetic layer or at the interfacial regions, the squareness of the magnetic transfer curve is calculated over a temperature range from 300 K to 5 K. Herein the squareness (Sq) is defined as,

$$Sq = \sqrt{\left(\frac{R_{ZF1} - R_m}{R_{AP} - R_m}\right) \times \left(\frac{R_m - R_{ZF2}}{R_m - R_P}\right)}, \quad R_m = \frac{R_P + R_{AP}}{2} \tag{2}$$

As shown in Fig. 4(a), R_{ZF1} and R_{ZF2} are the resistance values at zero magnetic field while R_P and R_{AP} are the resistance values in the P and AP magnetization configurations, respectively. The squareness is related to the existence of inhomogeneous regions in the free layer [21]. As displayed in Fig. 4(b), the large squareness (~0.9) suggests that there are few magnetic inhomogeneous regions or magnetic pinning sites existing in the free layer so that the magnetization of the free layer can switch uniformly with the external magnetic field. Therefore, the magnetic impurities are probably located at the interface rather than inside the free layer.

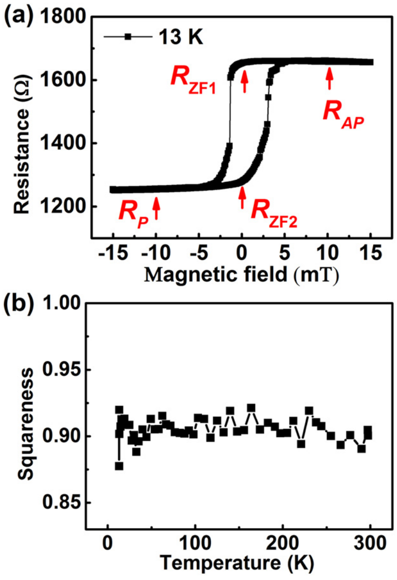

Fig. 4. (a) Typical magnetic transfer curve of the MTJ with junction area of 125 μm^2 measured at 13 K. (b) Temperature dependence of the squareness of the magnetic transfer curves.

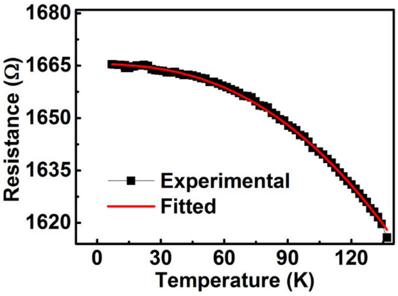

Fig. 5. Temperature dependence of R_{AP} of the MTJ with junction area of 125 μm^2 measured from 140 K to 5 K. The red solid line is the fitted curve using the GM model, $R_{AP}(T) = 1/G_{AP}(T) = 1/(A + BT^{1.33} + CT^{2.5} + DT^{3.6})$, where G_{AP} is the corresponding conductance in the AP state, the fitting parameters $A = 6.00 \times 10^{-4}\ \Omega^{-1}$, $B = 1.30 \times 10^{-9}\ \Omega^{-1}\,K^{-1.33}$, $C = 7.59 \times 10^{-11}\ \Omega^{-1}\,K^{-2.5}$, and $D = 1.15 \times 10^{-15}\ \Omega^{-1}\,K^{-3.6}$. (For interpretation of the references to color in this figure legend, the reader is referred to the web version of this article.)

The influence of the magnetization alignment on the Kondo effect was then studied. Fig. 5 shows R_{AP} as a function of temperature. As opposed to the temperature dependence of R_P, the $R_{AP}(T)$ curve can be fitted well with the GM model. In order to explain this behavior, the spin-flip nature of the Kondo scattering and its nontrivial impact on the tunneling process should be taken into account. To start with, the direct influence of the Kondo scattering on the tunneling current is considered while the spin-flip nature of the Kondo effect is not taken into consideration. In both the P and AP magnetization configurations, the injected electrons are scattered by the magnetic impurities located at the free layer/barrier interface, which diminishes the tunneling current. However, the spin-flip scattering associated with the Kondo effect contributes to the tunneling current in the P and AP magnetization configurations in an opposite manner [10]. For those electrons scattered by the magnetic impurities, the spin orientation of each electron is flipped due to the spin-exchange interaction between the electrons and the magnetic impurities. The majority spin is converted to the minority one and *vice versa*, which reduces the spin-polarization of the tunneling electrons. The decline of the polarization can then affect the tunneling current according to the conductance model developed by Shang's group [22]. The conductance values in the P and AP magnetization alignments are expressed as,

$$\begin{aligned} G_P(T) &= G_T(1 + P_1P_2) + \alpha T^{\frac{4}{3}}, \\ G_{AP}(T) &= G_T(1 - P_1P_2) + \alpha T^{\frac{4}{3}} \end{aligned} \tag{3}$$

Here G_T is the direct elastic tunneling term, α is a constant, and P_1 and P_2 are the effective polarizations of the free and pinned layers, respectively. The decrease of the spin-polarization suppresses the tunneling current for the P magnetization alignment but raises the tunneling current for the AP magnetization alignment. Therefore, in the P state, both the interfacial Kondo scattering and its resulting reduction of the spin polarization hinder the tunneling process and thus increase the junction resistance, enabling us to observe the Kondo effect. However, in the AP state, the spin-flip scattering associated with the Kondo effect has a nontrivial contribution to the tunneling current, which compensates the reduction of the tunneling current directly caused by the interfacial Kondo scattering, making the R^* contribution disappear. This experimental result is seemingly inconsistent with that reported previously in the literature [7,9], where the Kondo effect was also observed in the AP magnetization configuration. This dis-

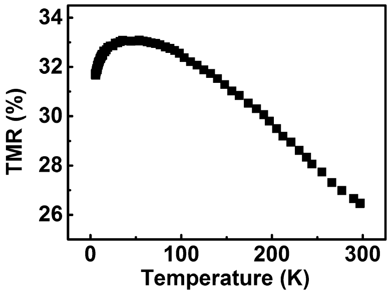

Fig. 6. Temperature dependence of TMR of the MTJ with junction area of 125 μm^2 measured from 300 K to 5 K.

crepancy can be explained by the difference in the concentration of magnetic impurities. The concentration of magnetic impurities is much higher in the earlier reported works than that in the MTJ we are investigating, which is suggested by the larger estimated Kondo resistivity ρ_0 in literature ([7]: 1.70×10^3 Ωm to 1.30×10^4 Ωm; [9]: 6.25×10^5 Ωm to 8.63×10^5 Ωm), compared with the calculated ρ_0 (∼3 Ωm) in this MTJ. As the concentration of magnetic impurities is extremely low, only one spin-flip scattering event is presumably involved for each scattered electron. The spins of the scattered electrons are then flipped, which reduces the spin-polarization of the tunneling electrons and thus suppresses the resistance in the AP state. This suppression of the resistance therefore compensates the increase of the resistance directly caused by scattering in this MTJ. However, since the concentration of magnetic impurities is much higher in the published literature [7,9], sequential spin-flip scattering events are probably involved and the flipped spins of electrons could be scattered back to their initial states. The decline of the spin-polarization caused by the former spin-flip scattering events could be canceled out by the later ones. Therefore, the influence of the spin-flip events tends to be diminished and the direct influence of scattering becomes dominant in the MTJs with much higher impurity concentration. As a result, the MTJ resistance is significantly raised in both the P and AP magnetization configurations in the previously reported works [7,9].

The Kondo effect activated at low temperature also diminishes the TMR of the MTJ. As shown in Fig. 6, above 40 K the TMR value gradually grows with the decreasing temperature, which is a typical behavior for a MTJ. Upon further reduction in temperature, the TMR curve exhibits an anomalous drop attributed to the increase of R_{P}, which is in line with those reported in the literature [7,9]. This phenomenon is believed to be another strong indicator evidencing the presence of the Kondo effect in the MTJ [7–9,23,24].

4. Conclusions

In this report, the manifestation of the Kondo effect in MTJs is demonstrated to be strongly dependent on the magnetization configuration. In the P magnetization configuration, both the direct effect of the interfacial Kondo scattering and the accompanied spin-flip process suppress the tunneling current below a critical temperature, leading to a nontrivial increase of the MTJ resistance. However, in the AP magnetization configuration, the spin-flip process promotes the tunneling of the conduction electrons, which compensates the suppression of the tunneling current caused by the Kondo scattering, making the additional resistance contribution disappear. These results indicate that the spin-flip process associated with the Kondo scattering plays a crucial role in determining the MTJ resistance, providing a possible route to manipulate the spin-dependent transport in MTJs. Also, the manifestation of the Kondo effect can be changed by altering the magnetization configuration of the MTJ. This behavior has not been experimentally observed before in a MTJ, although it was theoretically predicted in a quantum dot system [25]. Future work will focus on the impact of the spin-flip process on the zero-bias anomaly of the MTJs, which may serve as a powerful tool to probe more spin-dependent properties (g-factor, localized moments, spin-flip energy) of the magnetic impurities formed inside the system.

Acknowledgements

This work was supported in part by the Seed Funding Program for Basic Research and Small Project Funding Program from the University of Hong Kong, ITF Tier 3 funding (ITS/104/13, ITS/214/14), RGC-GRF grant (HKU 704911P), and University Grants Committee of Hong Kong (Contract No. AoE/P-04/08).

Appendix A. Supplementary material

Supplementary material related to this article can be found online at http://dx.doi.org/10.1016/j.physleta.2016.05.001.

References

[1] S. Zhang, S.B. Ogale, W. Yu, X. Gao, T. Liu, S. Ghosh, G.P. Das, A.T.S. Wee, R.L. Greene, T. Venkatesan, Electronic manifestation of cation-vacancy-induced magnetic moments in a transparent oxide semiconductor: anatase Nb:TiO$_2$, Adv. Mater. 21 (2009) 2282–2287.

[2] K.P. Wójcik, I. Weymann, Two-stage Kondo effect in T-shaped double quantum dots with ferromagnetic leads, Phys. Rev. B 91 (2015) 134422.

[3] S. Schmitt, F.B. Anders, Nonequilibrium Zeeman splitting in quantum transport through nanoscale junctions, Phys. Rev. Lett. 107 (2011) 056801.

[4] M.L. Perrin, E. Burzurí, H.S.J. van der Zant, Single-molecule transistors, Chem. Soc. Rev. 44 (2015) 902–919.

[5] L. O'Brien, M.J. Erickson, D. Spivak, H. Ambaye, R.J. Goyette, V. Lauter, P.A. Crowell, C. Leighton, Kondo physics in non-local metallic spin transport devices, Nat. Commun. 5 (2014) 4927.

[6] W.T. Herrera, Y.T. Xing, S.M. Ramos, P. Munayco, M.B. Fontes, E.M. Baggio-Saitovitch, F.J. Litterst, Kondo effect and spin-glass behavior of dilute iron clusters in silver films, Phys. Rev. B 84 (2011) 014430.

[7] K.I. Lee, S.J. Joo, J.H. Lee, K. Rhie, T.S. Kim, W.Y. Lee, K.H. Shin, B.C. Lee, P. LeClair, J.S. Lee, J.H. Park, Kondo effect in magnetic tunnel junctions, Phys. Rev. Lett. 98 (2007) 107202.

[8] D. Ciudad, Z.C. Wen, A.T. Hindmarch, E. Negusse, D.A. Arena, X.F. Han, C.H. Marrows, Competition between cotunneling, Kondo effect, and direct tunneling in discontinuous high-anisotropy magnetic tunnel junctions, Phys. Rev. B 85 (2012) 214408.

[9] S. Joo, K.Y. Jung, B.C. Lee, T.S. Kim, K.H. Shin, M.H. Jung, K.J. Rho, J.H. Park, J. Hong, K. Rhie, Effect of oxidizing the ferromagnetic electrode in magnetic tunnel junctions on tunneling magnetoresistance, Appl. Phys. Lett. 100 (2012) 172406.

[10] H. Yang, S.H. Yang, G. Ilnicki, J. Martinek, S.S.P. Parkin, Coexistence of the Kondo effect and a ferromagnetic phase in magnetic tunnel junctions, Phys. Rev. B 83 (2011) 174437.

[11] W.F. Egelhoff Jr., R.D. McMichael, C.L. Dennis, M.D. Stiles, A.J. Shapiro, B.B. Maranville, C.J. Powell, Suppression of orange-peel coupling in magnetic tunnel junctions by preoxidation, Appl. Phys. Lett. 88 (2006) 162508.

[12] B.B. Singh, S. Chaudhary, Effect of annealing on the temperature dependence of inelastic tunneling contributions vis-à-vis tunneling magnetoresistance and barrier parameters in CoFe/MgO/NiFe magnetic tunnel junctions, J. Appl. Phys. 115 (2014) 083904.

[13] T.P. Sarkar, K. Gopinadhan, M. Motapothula, S. Saha, Z. Huang, S. Dhar, A. Patra, W.M. Lu, F. Telesio, I. Pallecchi Ariando, D. Marre, T. Venkatesan, Unexpected observation of spatially separated Kondo scattering and ferromagnetism in Ta alloyed anatase TiO$_2$ thin films, Sci. Rep. 5 (2015) 13011.

[14] D. Goldhaber-Gordon, J. Göres, M.A. Kastner, H. Shtrikman, D. Mahalu, U. Meirav, From the Kondo regime to the mixed-valence regime in a single-electron transistor, Phys. Rev. Lett. 81 (1998) 5225–5228.

[15] I. Weymann, Finite-temperature spintronic transport through Kondo quantum dots: numerical renormalization group study, Phys. Rev. B 83 (2011) 113306.

[16] J.J. Parks, A.R. Champagne, T.A. Costi, W.W. Shum, A.N. Pasupathy, E. Neuscamman, S. Flores-Torres, P.S. Cornaglia, A.A. Aligia, C.A. Balseiro, G.K.L. Chan, H.D. Abruna, D.C. Ralph, Mechanical control of spin states in spin-1 molecules and the underscreened Kondo effect, Science 328 (2010) 1370–1373.

[17] J.J. Cha, M. Claassen, D. Kong, S.S. Hong, K.J. Koski, X.L. Qi, Y. Cui, Effects of magnetic doping on weak antilocalization in narrow Bi$_2$Se$_3$ nanoribbons, Nano Lett. 12 (2012) 4355–4359.

[18] P. Kharel, R. Skomski, P. Lukashev, R. Sabirianov, D.J. Sellmyer, Spin correlations and Kondo effect in a strong ferromagnet, Phys. Rev. B 84 (2011) 014431.

[19] C.P. Lin, C.Y. Hsu, S.J. Sun, H. Chou, The Kondo effect and carrier transport in amorphous Cr-doped In_2O_3 thin films, AIP Adv. 2 (2012) 042186.

[20] H. Yang, S.H. Yang, G. Ilnicki, J. Martinek, S.S.P. Parkin, Zero-bias anomaly in magnetic tunnel junctions, Acta Phys. Pol. A 118 (2010) 316–318.

[21] J.J. Kan, K. Lee, M. Gottwald, S.H. Kang, E.E. Fullerton, Low-temperature magnetic characterization of optimum and etch-damaged in-plane magnetic tunnel junctions, J. Appl. Phys. 114 (2013) 114506.

[22] C.H. Shang, J. Nowak, R. Jansen, J.S. Moodera, Temperature dependence of magnetoresistance and surface magnetization in ferromagnetic tunnel junctions, Phys. Rev. B 58 (1998) R2917–R2920.

[23] S.Y. Bae, S.X. Wang, Transport in magnetically doped magnetic tunnel junctions, IEEE Trans. Magn. 38 (2002) 2721–2723.

[24] H. Yang, S.H. Yang, S.S.P. Parkin, Crossover from Kondo-assisted suppression to co-tunneling enhancement of tunneling magnetoresistance via ferromagnetic nanodots in MgO tunnel barriers, Nano Lett. 8 (2008) 340–344.

[25] R. López, J.S. Lim, J. Martinek, P. Simon, Tunable Kondo effect in a double quantum dot coupled to ferromagnetic contacts, Phys. Rev. Lett. 108 (2012) 166605.